CHAPTER IV
CATALYTIC ACTIVITY STUDY OF Fe, Ti LOADED TUD-1

4.1 Abstract

Bimetallic Fe and Ti incorporated into TUD-1 framework is successfully synthesized by sol–gel method. Tetraethyl ammonium hydroxide (TEAOH) was used as a structural directing agent. Silatrane, iron (III) chloride hexahydrate, and titanium (IV) isopropoxide were utilized as the silica, iron, and titanium sources, respectively. The synthesized Fe,Ti-TUD-1 was characterized by XRD, N_2 adsorption/desorption, XRF, and DRUV. The obtained material has disordered mesoporous structures with high surface area (708–769 m^2/g). To study the catalytic activity of the synthesized Fe,Ti–TUD-1, phenol hydroxylation using hydrogen peroxide as oxidizing agent was selected as a model reaction. Many factors were investigated, including reaction temperature, reaction time, amount of metals loaded, amount of catalyst, and molar ratio of reactants. The catalytic activity and selectivity of phenol hydroxylation were studied, and showed the high phenol conversion up to 93% with the selectivity of hydroquinone reached 53% at 90 °C for 1 h, using 30 mg of 0.01Fe,0.01Ti-TUD-1 catalyst and 1:3 phenol:H_2O_2.

Keywords: Silatrane, TUD-1, Bimetallics, Iron, Titanium, Phenol hydroxylation, Sol-gel process

4.2 Introduction

TUD-1, one type of mesoporous silica, was discovered by the researcher from Lummus Technology and the Delft University of Technology in 2001 [1]. It possesses a three-dimensional amorphous structure of random and interconnecting pores. Unlike most other mesoporous materials, TUD-1 has many characteristics that make it a promising material as the catalyst. For instance, it has a high surface area (400–1000 m^2/g), an excellent hydrothermal stability, a tunable pore size, and a better diffusion of large molecules into and out of the pores [2, 3]

The first synthesis route uses tetraethylorthosilane (TEOS) as the monomeric silica source mixing with triethanolamine (TEA) and optionally tetraethylammonium hydroxide (TEAOH). TEAOH acts as a template while TEA acts as co-template for both meso- and some micropore formation. Moreover, TEAOH generates a basic environment to accelerate TEOS hydrolysis [2].

According to material safety data sheet (MSDS), TEOS has significant disadvantages, such as high toxicity and moisture sensitivity. In order to solve these problems, the moisture stable and inexpensive silica source, silatrane introduced by Wongkasemjit's research group was used instead. It allows controlling the hydrolysis rate during sol-gel process. In addition, after silatrane is hydrolyzed, it generates TEA molecules, which act as the directing agent for TUD-1. Thus, it should be an important benefit of using this precursor [4-7].

However, the pure silica TUD-1 limits its catalytic applications. Incorporation of metals including most of the transition metals and some main group elements, such as boron, gallium and indium etc. into the frameworks of mesoporous materials is thus studied to modify the composition and improve its catalytic activity of the materials [8,9]. Moreover, the incorporation of multi-component of hetero atoms can modify the surface properties more effectively than those of mono-kind of heteroatom and could be widely used in the field of catalysis [8].

In this research, the objectives of this work are to synthesize bimetallic Fe/Ti loaded TUD-1 material via a sol-gel technique using silatrane as a precursor, and to study catalytic activity on oxidation of phenol due to its valuable oxidation products, viz. catechol (CAT), hydroquinone (HQ), and 1,4-benzoquinone (BQ). In

many researches, titanium and iron are widely loaded in many mesoporous silica and are tested as catalysts for this reaction, including Ti-MSU [10], Ti-SBA-12, Ti-SBA-16 [11], Fe-MCM-48 [12], Fe-MCM-41 [13], and Fe-HMS [14]. Many factors are also studied to find the optimum condition, such as reaction temperature, reaction time, amount of metals loaded, amount of catalyst, and molar ratio of reactants. Moreover, leaching, recycling, thermal stability of the catalyst, and photocatalytic reaction are studied, as well.

4.3 Experimental

4.3.1 Materials

Fumed silica (SiO_2, 99.8%, Nippon Aerosil, Japan), UHP grade nitrogen (N_2, 99.99% purity, Thai Industrial Gases Public Company Limited (TIG), Thailand), ethylene glycol (EG, 99%, J.T. Baker, USA), TEA (QRëc chemical, Thailand), acetonitrile (CH_3CN, 99.9%, Labscan, Thailand), methanol (CH_3OH, 99.9%, Labscan, Thailand), TEAOH (35% in water) (Sigma-Aldrich, USA), CAT (99%, Sigma-Aldrich, USA), HQ (99%, Sigma-Aldrich, USA), BQ (98%, Sigma-Aldrich, USA), phenol detached crystals (Fisher scientific, UK), hydrogen peroxide (H_2O_2, 30% w/v, Fisher scientific, UK), iron (III) chloride hexahydrate ($FeCl_3.6H_2O$, Sigma-Aldrich, USA), and titanium (IV) isopropoxide (98%, Acros organics, USA) were used without further purification.

4.3.2 Synthesis Method

4.3.2.1 Synthesis of Silatrane

Wongkasemjit's synthetic method was followed by mixing fumed silica (0.1 mol), EG (100 ml), and TEA (0.125 mol) [15]. The mixture was refluxed at 200 °C under N_2 atmosphere for 10 h in oil bath. The excess EG and water were removed under vacuum at 100 °C. The product was washed by acetronitrile to remove TEA and EG residue. The silatrane product was vacuum-dried overnight before characterization using TGA and FT-IR.

4.3.2.2 Synthesis of Fe,Ti Loaded TUD-1

The synthesis of Fe,Ti-TUD-1 was carried out according to Wongkasemjit's method [16]. A desired amount of $FeCl_3.6H_2O$ was dissolved in de-ionized water and the solution was stirred continuously, followed by adding silatrane precursor into the mixture. After that titanium (IV) isopropoxide was slowly added, the mixture was stirred for 1 h, followed by slow introduction of TEAOH. The mixture was aged at room temperature for 4 h before drying at 100 °C for 24 h. The molar ratio of the mixture was 1.0 silatrane:14H_2O:0.7TEAOH:xTi,yFe, where $0.01 \leq x, y \leq 0.09$. The resulting material was calcined at 600 °C for 10 h using a heating rate of 1 °C/min. Si-TUD-1, Fe-TUD-1 and Ti-TUD-1 were also synthesized using the same procedure as the bimetallic TUD-1, for comparison.

4.3.3 Materials Characterization

The phase of mesoporous products was characterized on a Rigaku TTRAX III Small Angle X-Ray Diffraction (SAXD) with a scanning speed of 1 °/min and CuKα source (λ= 0.154 Å) in a range of 2θ = 0.4–8°. Wide Angle X-Ray Diffraction (WAXD) was performed on a Rigaku Smartlab® with a scanning speed of 10 °/min and CuKα source (λ= 0.154 Å) in a range of 2θ = 20–80° to determine the metal nanocrystals. The specific surface area was measured by the Brunauer-Emmett-Teller (BET) method and the pore size distribution was calculated by the Barrett-Joyner-Halenda (BJH) on a Quantasorb Jr. (Autosorb-1). Prior to each analysis, the product was degassed at 250 °C for 12 h. Thermal properties were analyzed by Thermal gravimetric analysis-Fourier transform infrared spectrometry (TGA-FTIR) on Pyris Diamons Perkin Elmer using a heating rate of 10 °C/min under N_2 atmosphere. FTIR analysis was conducted on a Perkin Elmer (Spectrum One) with a scanning resolution of 4 cm^{-1} to investigate functional groups of the synthesized precursors. Powder specimens contained 1.0% sample with 99% potassium bromide (KBr). Identification of Fe,Ti loaded TUD-1 framework was observed by Diffused reflectance ultraviolet-visible spectrometer (DRUV) on a Shimadzu UV-2550 using $BaSO_4$ as the reference. The metal contents in samples were observed by X-ray fluorescence (XRF) on AXIOS PW 4400.

4.3.4 Activity Study

The study was followed Adam and coworkers' method [17] for the oxidation of phenol by dissolving phenol (1.88 g, 20 mmol) in 10 mL of water. The mixture was then transferred into in a 50 mL double-necked round-bottom flask fitted with a water-cooled condenser, containing 30 mg of catalyst and immersing in an oil bath was added drop-wise to the vigorously stirred (600 rpm) reaction mixture. Aliquots of the reaction mixture (0.5 cm^3) were periodically withdrawn using a syringe. The samples were analyzed by a UFLC Shimadzu high performance liquid chromatography (HPLC) equipped with a C-18 reverse-phase column (Inertsil ODS-3) and a UV detector (SPD-M20A Shimadzu). The products were further confirmed by comparing the HPLC of the respectively pure CAT, BQ, and HQ. All reactions were performed in triplicate and average values were used in the data presentation [17].

4.3.5 Leaching and Reusable Study

Leaching of metal ions from the catalyst was determined by filtering off the catalyst from the reaction mixture after 30 min by using hot filtration technique. The hot filtrate was transferred without delay into a round bottom flask which had been immersed in oil bath at the same temperature. The reaction was allowed to continue for 1 h (without the catalyst) and the course of the reaction was monitored periodically by HPLC-UV to compare with the results before hot filtration [17].

Reusability was studied by regenerating the catalyst by washing with distilled water, dried in an oven at 353K for 6 h and calcined at 500 °C for 2 h with a 0.5 °C/min heating rate. The catalyst was collected and reused for further runs, as described elsewhere [17].

4.4 Results and Discussion

4.4.1 Characterization of Silatrane Precursor

Silatrane precursor was identified by FT-IR and TGA. The results obtained were consistent with those reported previously [15]. The observed FT-IR bands were 3000–3700 cm^{-1} (w, νO–H), 2860–2986 cm^{-1} (s, νC–H), 1244–1275 cm^{-1} (m, νC–N), 1170–1117 cm^{-1} (bs, νSi–O), 1093 cm^{-1} (s, νSi–O–C), 1073 cm^{-1} (s, νC–O), 1049 cm^{-1} (s, νSi–O), 1021 cm^{-1} (s, νC–O), 785 and 729 cm^{-1} (s, νSi–O–C), and 579 cm^{-1} (w, νN-Si), as seen in Figure 4.1. TGA result in Figure 4.2 showed one sharp mass loss at 390 °C and gave a 19% ceramic yield of $N(CH_2CH_2O)_3Si–OCH_2CH_2–N(CH_2CH_2OH)_2$.

4.4.2 Characterization of Fe,Ti-TUD-1 Catalyst

XRD patterns of the calcined pure TUD-1 and metal loaded TUD-1 (Figure 4.3) showed a single broad peak at 2θ 0.8–2°, confirming the disorder mesostructured material of TUD-1 [18]. Ti-TUD-1 samples with Ti/Si ratio between 0.01 and 0.09 (Figure 4.3(c)) were successfully prepared using titanium(IV)isopropoxide as a titanium source due to the hydrophobic interaction between isopropoxide and TEAOH, which stabilized the structure of TUD-1 [19]. However, in case of Fe-TUD-1, further increase of Fe/Si ratio over 0.03 (Figure 4.3(b)) caused the TUD-1 structure collapsed because of the less effective anionic chloride ion of the iron precursor, causing an imbalance of the charge matching at high concentration [20]. Bimetallic samples of xFe-yTi-TUD-1with $0.01 \leq x \leq 0.03$ and $0.01 \leq y \leq 0.09$ (Figure 4.3(a)) also provided disorder mesostructured of TUD-1 with the absence of the characteristic peaks of TiO_2 and Fe_2O_3 nanoparticles, as observed by wide angle XRD (Figure 4.4).

N_2 Adsorption/desorption isotherms in Figure 4.5 showed a type IV isotherm with a typical H-2 hysteresis loop. It means that all TUD-1 samples had mesoporous structure with interconnected pore network [19]. Pure TUD-1, monometallic TUD-1, and bimetallic TUD-1 all exhibited the narrow pore size distribution with a pore diameter around 4.5–7.0 nm as shown in Figure 4.6. The physico-chemical properties of all TUD-1 samples were summarized in Table 4.1.

The BET surface area was obtained in a range of 562–777 m^2/g with a pore volume between 0.63–1.12 cc/g. In addition, the surface area and pore volume of metal loaded TUD-1 were higher than the pure TUD-1. The reason may come from the larger pore volume of the metal loaded TUD-1 than the pure TUD-1 due to the presence of the large iron (Paulling radius = 64 pm) and titanium atoms (Paulling radius = 60 pm), compared with the silicon atom (Paulling radius = 42 pm), in the framework, as explained by Ramanathan and co-workers [21].

The total amounts of the metal in Fe-TUD-1, Ti-TUD-1, and Fe-Ti-TUD-1 were also determined using XRF spectroscopy, as summarized in Table 4.2. It is revealed that the actual contents of Fe and Ti introduced into the framework of TUD-1 were closed to the composite gels.

The incorporation of Ti and Fe into the TUD-1 framework was examined by DRUV-Vis spectroscopy (Figure 4.7). Fe-TUD-1 samples with Fe/Si ratios of 0.01 and 0.03, as illustrated in Figure 4.7(a), showed the absorption band between 200 and 280 nm with a maximum centered at 240 nm, attributed to the charge-transfer transitions involving isolated Fe^{3+} in $Fe^{3+}O_4$ tetrahedral coordination. The adsorption band between 300 and 400 nm observed for the Fe-TUD-1 are attributed to octahedral Fe^{3+} in small oligomeric Fe_xO_y clusters. In addition, the band at 400–600 nm was also presented in the Fe-TUD-1 samples, indicating that these samples had the bulk iron oxide as the extraframework [22]. Ti-TUD-1 samples (Figure 4.7(a)) showed an intense UV band at 200 nm, which was characteristic of the tetrahedral titanium sites in the framework, which are known as the catalytic active site for the reactions. However, as the Ti/Si ratio increased above 0.01, a broad band in the region from 220 to 260 nm, corresponding to partially polymerized Ti–O–Ti species, appeared. Moreover, octahedral anatase was also detected at 330 nm [16]. The bimetallic Fe and Ti loaded TUD-1 (Figure 4.7(b)) exhibited the band at 200 nm related to the tetrahedral coordinations of isolated Fe^{3+} and Ti^{4+}. The absorption bands of some Ti-O-Ti species, small Fe-O-Fe clusters and octahedral ferric oxide extraframework were observed at 250–300, 300–400, and 400–600 nm, respectively. The energy band gaps of the tetrahedral Fe^{3+} and Ti^{4+} calculated from equation 4.1 are 5.18 and 6.21 eV, respectively.

$$\text{Band gap energy } (E) = h^{*}C/\lambda \qquad (4.1)$$

Where h = Planks constant = 6.626×10^{-34} Joules sec

C = Speed of light = 3.0×10^{8} meter/sec

λ = Cut off wavelength (meter)

1eV = 1.6×10^{-19} Joules

4.4.3 Catalytic Activity on Phenol Hydroxylation

To obtain the optimum condition of the reaction, the following factors were studied.

4.4.3.1 Reaction Temperature

The reaction temperature was varied from 30–90 °C, as presented in Figures 4.8 and 4.9. The optimum reaction temperature was chosen by consideration of the temperature giving the most desirable phenol conversion and selectivity. It was observed that the phenol conversion increased with temperature from 30.8 to 59.7% within 1 h. In addition, when the temperature went up to 90 °C, BQ disappeared while HQ selectivity increased to 53.1%. This indicates that BQ is energetically activated before converting to a higher energy molecule as HQ [23]. Thus, 90 °C was selected as the optimum reaction temperature.

4.4.3.2 Reaction Time

At the optimum temperature, the phenol conversion increased rapidly and reached equilibrium within 30 min due to the fast decomposition of H_2O_2 at high temperature [17]. The reaction at 30 min showed 61.0% of phenol conversion and yielded only HQ and CAT products with 50.2% selectivity of HQ, as shown in Figure 4.8. Figure 4.9 shows that the BQ selectivity was 11.0% at the beginning of the reaction and gradually decreased to 0% after 30 min. The similar result was also observed by Sun and co-workers [24] who found that the selectivity of BQ in the product was very high at the beginning of the reaction. As prolonging the reaction beyond 4 h, BQ selectivity was down to 2.3%. The reason may come from the fact that the formation of para-BQ was a fast over-oxidation of HQ in the reaction medium by a large concentration of H_2O_2 at the beginning of the reaction, as

described by Allian and co-workers [25]. In this study, 60 min reaction time was chosen as the optimum reaction time because of the higher product selectivity of HQ.

4.4.3.3 Amount of Catalyst

The effect of the catalyst mass was studied using various catalyst contents (10 to 70 mg), as shown in Figure 4.10. The maximum phenol conversion of 53.8% was obtained when 30 mg of catalyst was used. Further increase in the catalyst mass to 70 mg, the conversion was slightly decreased to 50.1%. The reason was explained by Adam and co-workers [17]. It could be that the larger amount of catalyst accelerated the H_2O_2 dissociation, causing too fast reaction rate to form the active intermediate that affects the oxidation [17]. The overall reactions and the reaction of the active intermediate formation are described in Scheme 4.1, 4.2 and 4.3-4.4, respectively [13, 26-27]. In contrast, the product selectivity of HQ was maximized when the catalyst content was 70 mg. Since the conversion was decreased as increasing the catalyst content to 70 mg, the optimum catalyst mass selected was 30 mg.

4.4.3.4 Reactants Molar Ratio

The molar ratio of phenol to H_2O_2 was studied and the results are presented in Figure 4.11. The phenol conversion was found to increase dramatically with an increase in H_2O_2 amount from 53.8 to 90.5% (for 1:1 and 1:3 phenol:H_2O_2, respectively). When the molar concentration of H_2O_2 was fixed and the molar concentration of the phenol was increased, the phenol conversion was decreased to 38.0% due to insufficient amount of H_2O_2 to react with the large excess of phenol, as explained by Adam and coworkers [17]. The product selectivity was found to remain constant at 55.0% of HQ and 45.0% of CAT throughout the molar ratio variation of the reactants studied. It can be concluded that the optimum molar ratio was 1:3 phenol:H_2O_2.

4.4.3.5 Amount of Metal Loaded

The effect of the metal loading (Table 4.3) was studied under the optimum reaction conditions. All metal loaded TUD-1 showed the higher phenol conversion than the pure TUD-1. 0.01Fe,0.01Ti-TUD-1 exhibited high phenol conversion at 93.1% with the 53.4% HQ selectivity. Its catalytic activity was almost the same as that of 0.01Fe-TUD-1. Likewise, 0.03Fe,0.01Ti-TUD-1, which had the

lower phenol conversion, but higher BQ selectivity than those using the 0.01Fe,0.01Ti-TUD-1, also showed the similar catalytic activity to 0.03Fe-TUD-1. From the DRUV results, the Fe/Si > 0.03 resulted in some polymerized Fe species in the extraframework, and these species can accelerate a decomposition of H_2O_2, making the phenol conversion decrease [14]. Moreover, the smaller catalytic active sites could reduce the dihydroxybenzene selectivity [13, 14]. Although further increase in the titanium loading of bimetallic catalysts leaded to a decrease in the catalytic activity, the bimetallic TUD-1 still showed the higher conversion than Ti-TUD-1. This was also accompanied with a fall in the dihydroxybenzene selectivity, but the increase in BQ selectivity. The similar reason was explained in the same way as the Fe species, which was discussed by Perego and co-workers [28]. Hence, the optimum metal loading of bimetallic TUD-1 chosen was 0.01Fe,0.01Ti-TUD-1.

4.4.3.6 Leaching and Catalyst Recycling

Leaching effect and catalyst reusability were performed by using 0.01Fe,0.01Ti-TUD-1 due to its highest phenol conversion. The results showed that after the catalyst was filtered by hot filtration for 30 min, the phenol conversion was significantly increased as the reaction time increased, as presented in Table 4.4. It indicated that the extraframework Fe which was retained in the support only by weak Van der Waals bonds, leached out to the reaction mixture [29]. Moreover, strong complexing and solvolytic properties of the oxidant and/or intermediate products (e.g. catechol) may rupture the metal-oxygen bonds, resulting in the metal leaching [29]. The leaching result was confirmed by the dramatic decrease of phenol conversion for the second and the third recycling cycle, as shown in Table 4.5. The third reused catalyst was characterized by SAXD and SAA, as shown in Figure 4.12 and Table 4.6, respectively. The results showed the disappearance of the characteristic peak of TUD-1 and the decrease of the BET surface area. This is an indicative of the collapse in the catalyst structure.

4.4.3.7 Hydrothermal Stability

To study the hydrothermal stability of the catalyst, the used 0.01Fe-TUD-1, 0.01Ti-TUD-1, and 0.01Fe,0.01Ti-TUD-1 were rinsed with water and calcined at 500 °C with a heating rate 0.5 °C/min for 2 h to remove the organic residue. The calcined catalyst was examined by SAXD and SAA, as illustrated in

Figure 4.12 and Table 4.6, respectively. The results showed that the BET surface area of the used catalysts decreased. The characteristic peak of the bimetallic catalyst was disappeared. However, monometallic catalyst still exhibited the characteristic peak of TUD-1. The less hydrothermal stability of bimetallic TUD-1 may come from the larger pore size than the monometallic TUD-1, as shown in Table 4.1, resulting in the less wall thickness, which is one of the factors responsible for their hydrothermal stability [30].

4.4.3.8 Photocatalytic Reaction

Table 4.7 shows the photocatalytic activity of the monometallic and bimetallic TUD-1 for phenol hydroxylation which was performed under 100 W of UV radiation. Both pure TUD-1 and 0.01Ti-TUD-1 had low photocatalytic activity. However, titanium modified samples exhibit the activity as a function of titanium loading. The highest activity was observed at 0.07% of Ti/Si. A further increase in titanium loading resulted in a decrease of activity, possibly due to a combination of factors including decrease in surface area, pore size and increase in TiO_2 particle size inside the channels [31]. The similar result was also observed in bimetallic TUD-1. Moreover, the increase in iron content did not improve the photocatalytic activity for both monometallic and bimetallic TUD-1, indicating that the incorporation of titanium species enhanced the photocatalytic activity.

4.5 Conclusions

The bimetallic Fe,Ti-TUD-1 was successfully synthesized via sol-gel process using silatrane, titanium(IV)isopropoxide and iron(III)chloride as silica, titanium, and iron sources, respectively. The obtained 0.01Fe,0.01Ti-TUD-1 was utilized as the catalyst for phenol hydroxylation, using the following optimum conditions: 90 °C reaction temperature, 60 min reaction time, 1:3 phenol:hydrogen peroxide ratio, and 30 mg of catalyst content. The highest phenol conversion of 93.1% with the 53.4% selectivity of hydroquinone was obtained. However, leaching of the metal ion into the reaction mixture was observed, making the catalyst unable to be reused. The thinner wall thickness of 0.01Fe,0.01Ti-TUD-1 showed the lower hydrothermal stability than 0.01Fe-TUD-1 and 0.01Ti-TUD-1, having the thicker

wall. The phenol hydroxylation under the UV radiation showed the lower phenol conversion (17.4%).

4.6 Acknowledgments

This research work is supported by the Development and Promotion of Science and Technology Talent Project (DPST), Ratchadapisake Sompote Endowment Fund, Thailand Research Fund, the Petroleum and Petrochemical College and the Center of Excellence on Petrochemical and Materials Technology, Chulalongkorn University, Thailand.

4.7 References

1. Jansen, J. C., Shan, Z., Marchese, L., Zhou, W., Puil, N. v. d., Maschmeyer, T. (2001) A new templating method for three-dimensional mesopore networks. Chemical Communications, 713 –714.
2. Angevine, P.J., Gaffney, A.M., Shan, Z., Koegler, J.H., Yeh, C.Y. "TUD-1: A generalized mesoporous catalyst family for industrial applications." Digital Refining. Dec 2008. 10 May 2013 <www.digitalrefming.com/article/1000209>
3. Telalović, S., Ramanathan, A., Mul, G., Hanefeld, U. (2009). TUD-1: synthesis and application of a versatile catalyst, carrier, material. Journal of Materials Chemistry, 20, 642–658.
4. Longloilert, R., Chaisuwan, T., Luengnaruemitchai, A., Wongkasemjit, S. (2011) Synthesis of MCM-48 from silatrane via sol–gel process. Journal of sol-gel science and technology, 58, 427-435.
5. Samran, B., White, T. J., Wongkasemjit, S. (2011) A novel room temperature synthesis of mesoporous SBA-15 from silatrane. Journal of Porous Materials, 18, 167-175.
6. Tanglumlert, W., Imae, T., White, T. J., Wongkasemjit, S. (2007) Structural aspects of SBA-1 cubic mesoporous silica synthesized via a sol-gel process using silatrane precursor. Journal of the American Ceramic Society, 90(12), 3992–3997.

7. Thanabodeekij, N., Tanglumlert, W., Gulari, E., Wongkasemjit, S. (2005) Synthesis of Ti-MCM-41 directly from silatrane and titanium glycolate and its catalytic activity. Applied Organometallic Chemistry, 19, 1047-1054.
8. Wu, Y., Zhang, Y., Cheng, J., Li, Z., Wang, H., Sun, Q., Han, B., Kong, Y. (2012) Synthesis, characterization and catalytic activity of binary metallic titanium and iron containing mesoporous silica. Microporous and Mesoporous Materials, 162, 51–59.
9. Kustrowski, P., Chmielarz, L., Dziembaj, R., Cool, P., Vansant, E.F. (2005) Modification of MCM-48-, SBA-15-, MCF-, and MSU-type mesoporous silicas with transition metal oxides using the molecular designed dispersion method. The Journal of Physical Chemistry B, 109, 11552–11558.
10. Song S., Zhao, W., Wang, L., Chu, J., Qu, J., Li, S., Wang, L., Qi, T. (2011) One-step synthesis of Ti-MSU and its catalytic performance on phenol hydroxylation. Journal of Colloid and Interface Science, 354, 686–690.
11. Kumar, A., Srinivas, D. (2013) Hydroxylation of phenol with hydrogen peroxide catalyzed by Ti-SBA-12 and Ti-SBA-16. Journal of Molecular Catalysis A: Chemical, 368– 369, 112– 118.
12. Zhao, W., Luo, Y., Deng, P., Li, Q. (2010) Synthesis of Fe-MCM-48 and its catalytic performance in phenol hydroxylation. Catalysis Letters, 73, 2-4.
13. Choi, J.-S., Yoon, S.-S., Jang, S.-H., Ahn, W.-S. (2006) Phenol hydroxylation using Fe-MCM-41 catalysts. Catalysis Today, 111, 280-287.
14. Liu, H., Lu, G., Guo, Y., Guo, Y., Wang, J. (2008) Study on the synthesis and the catalytic properties of Fe-HMS materials in the hydroxylation of phenol. Microporous and Mesoporous Materials, 108, 56–64.
15. Charoenpinijkarn, W., Sawankruhasn, M., Kesapabutr, B., Wongkasemjit, S., Jamieson, A.M. (2001) Sol-gel processing of silatranes. European Polymer Journal, 37, 1441-1448.

16. Tanglumlert, W., Yang, S.-T., Jeong, K.-E., Jeong, S.-Y., Ahn, W.-S. (2011) Facile synthesis of Ti-TUD-1 for catalytic oxidative desulfurization of model sulfur compounds. Research on Chemical Intermediates, 37, 1267–1273.
17. Adam, F., Andas, J., Rahman, I.A. (2010) A study on the oxidation of phenol by heterogeneous iron silica catalyst. Chemical Engineering Journal, 165, 658–667.
18. Shan, Z., Jansen, J.C., Marchese, L., Maschmeyer, Th. (2001) Synthesis, characterization and catalytic testing of a 3D mesoporous titanosilica, Ti-TUD-1. Microporous and Mesoporous Materials, 48, 181-187.
19. Zhang, Z.-X., Bai, P., Xu, B., Yan, Z.-F. (2006) Synthesis of mesoporous alumina TUD-1 with high thermostability. Journal of Porous Materials, 13, 245–250.
20. Mahoney, LM. (2010) Photocatalysis studies using mesoporous modified V-MCM-48 Stober synthesis. PhD thesis, Kansas State University, Kansas, USA.
21. Ramanathan, A., Villalobos, M. C. C., Kwakernaak, C., Telalovic, S., Hanefeld, U. (2008) Zr-TUD-1: a lewis acidic, three-dimensional, mesoporous, zirconium-containing catalyst. Chemistry- A European Journal, 14, 961-72.
22. Haddoum, S., Fechete, I., Donnio, B., Garin, F., Lutic, D., Chitour, C. E. (2012) Fe-TUD-1 for the preferential rupture of the substituted C-C bond of methylcyclopentane (MCP). Catalysis Communications, 27, 141–147.
23. Klaewkla, R., Rirksomboon, T., Kulprathipanja, S., Nemeth, L., Rangsunvigit, P. (2006) Light sensitivity of phenol hydroxylation with TS-1. Catalysis Communications, 7, 260–263.
24. Sun, J., Meng, X., Shi, Y., Wang, R., Feng, S., Jiang, D., Xu, R., Xiao, F.-S. (2000) A Novel Catalyst of Cu–Bi–V–O Complex in Phenol Hydroxylation with Hydrogen Peroxide. Journal of Catalysis, 193, 199–206.
25. Allian, M., Germain, A., Figueras, F. (1994) The formation of para-benzoquinone and the mechanism of the hydroxylation of phenol by hydrogen peroxide over solid acids. Catalysis Letters, 28, 409-415.
26. Qiao, J.-Q., Yuan, N., Tang, C.-J., Yang, J., Zhou, J., Lian, H.-Z., Dong, L. (2012) Determination of catalytic oxidation products of phenol by RP-HPLC. Research on Chemical Intermediates, 38, 549–558.

27. Wilkenhoner, U., Langhendries, G., van Laar, F., Baron, G.V., Gammon, D.W., Jacobs, P.A., van Steen, E. (2001) Influence of pore and crystal size of crystalline titanosilicates on phenol hydroxylation in different solvents. Journal of Catalysis, 203, 201–212.

28. Perego, C., Carati, A., Ingallina, P., Mantegazza, M. A., Bellussi, G. (2001) Production of titanium containing molecular sieves and their application in catalysis. Applied Catalysis A: General, 221, 63-72.

29. Crowther, N., Larachi, F. (2003) Iron-containing silicalites for phenol catalytic wet peroxidation. Applied Catalysis B: Environmental, 46, 293–305.

30. Timofeeva, M.N., Mel'gunov, M.S., Kholdeeva, O.A., Malyshev, M.E., Shmakov, A.N., Fenelonov, V.B. (2007) Full phenol peroxide oxidation over Fe-MMM-2 catalysts with enhanced hydrothermal stability. Applied Catalysis B: Environmental, 75, 290–297.

31. Zhao, S., Su, D., Che, J., Jiang, B., Orlov, A. (2011) Photocatalytic properties of TiO_2 supported on SBA-15 mesoporous materials with large pores and short channels. Materials Letters, 65, 3354–3357.

Table 4.1 The BET analysis of TUD-1 and metal loaded TUD-1 containing different metal contents

Samples	BET Surface Area (m^2/g)	Pore Volume (cc/g)	Average Pore Size (nm)
TUD-1	562	0.63	4.51
0.01-Ti-TUD-1	706	0.88	4.99
0.03-Ti-TUD-1	718	0.93	5.19
0.05-Ti-TUD-1	777	0.95	4.90
0.07-Ti-TUD-1	768	0.92	4.81
0.09-Ti-TUD-1	745	0.85	4.59
0.01-Fe-TUD-1	741	1.05	5.69
0.03-Fe-TUD-1	579	1.01	6.95
0.01Fe,0.01Ti-TUD-1	711	1.04	5.84
0.01Fe,0.03Ti-TUD-1	769	1.07	5.55
0.01Fe,0.05Ti-TUD-1	745	1.07	5.77
0.01Fe,0.07Ti-TUD-1	767	1.06	5.52
0.01Fe,0.09Ti-TUD-1	746	1.02	5.45
0.03Fe,0.01Ti-TUD-1	708	1.12	6.33

Table 4.2 The XRF analysis of Fe-TUD-1, Ti-TUD-1 and bimetallic Fe,Ti-TUD-1

Sample	Fe/Si (mole ratio)		Ti/Si (mole ratio)	
	Gel	Product*	Gel	Product*
TUD-1	0	0	0	0
0.01Fe-TUD-1	0.01	0.014	0	0
0.03Fe-TUD-1	0.03	0.033	0	0
0.01Ti-TUD-1	0	0	0.01	0.011
0.03Ti-TUD-1	0	0	0.03	0.037
0.05Ti-TUD-1	0	0	0.05	0.059
0.07Ti-TUD-1	0	0	0.07	0.079
0.09Ti-TUD-1	0	0	0.09	0.101
0.01Fe-0.01Ti-TUD-1	0.01	0.012	0.01	0.011
0.01Fe-0.03Ti- TUD-1	0.01	0.012	0.03	0.032
0.01Fe-0.05Ti- TUD-1	0.01	0.014	0.05	0.065
0.01Fe-0.07Ti-TUD-1	0.01	0.013	0.07	0.088
0.01Fe-0.09Ti-TUD-1	0.01	0.013	0.09	0.110
0.03Fe-0.01Ti-TUD-1	0.03	0.031	0.01	0.010

* Data were obtained from XRF.

Table 4.3 Effect of the metal loading on phenol hydroxylation (Thermal reaction)

Sample	conversion	Selectivity		
		HQ	CAT	BQ
TUD-1	3.49±1.81	-	16.88±4.95	83.12±4.95
0.01Fe-TUD-1	93.15±0.87	55.79±0.83	44.21±0.83	-
0.03Fe-TUD-1	26.47±5.40	35.35±3.12	54.84±1.73	9.81±1.47
0.01Ti-TUD-1	8.31±5.32	22.25±3.33	36.15±3.37	41.60±2.03
0.03Ti-TUD-1	10.07±0.35	26.67±3.72	35.05±1.12	38.28±4.79
0.05Ti-TUD-1	10.55±0.49	15.68±3.54	10.82±1.27	73.50±4.81
0.07Ti-TUD-1	11.23±0.84	15.82±0.35	6.89±1.13	77.29±1.38
0.09Ti-TUD-1	13.64±1.77	0.71±0.28	0.78±0.25	98.51±0.33
0.01Fe0.01Ti-TUD-1	93.06±0.24	53.40±0.77	46.60±0.77	-
0.01Fe0.03Ti-TUD-1	90.53±0.32	54.98±0.17	45.02±0.17	-
0.01Fe0.05Ti-TUD-1	40.52±11.09	35.09±1.03	60.85±1.22	4.06±0.20
0.01Fe0.07Ti-TUD-1	25.18±3.97	34.80±2.51	52.40±2.61	12.80±0.81
0.01Fe0.09Ti-TUD-1	14.57±1.35	24.16±3.95	46.81±0.50	29.03±3.48
0.03Fe0.01Ti-TUD-1	28.20±1.80	30.04±1.97	57.66±0.29	12.30±2.05
No H_2O_2	-	-	-	-
No catalyst	2.19±0.43	-	7.69±2.74	92.31±2.74

*The reaction performed at 90 °C for 1 h using 30 mg of catalyst and 1:3 phenol:H_2O_2 ratio.

Table 4.4 Study on the catalyst leaching of bimetallic Fe.Ti-TUD-1 after washing with hot water for 30 min

Time	Conversion	Selectivity		
		HQ	CAT	BQ
30m	31.40±3.30	17.33±1.84	36.48±2.64	46.18±4.48
40m	36.31±5.41	20.89±1.58	40.24±1.83	38.87±3.41
50m	60.30±6.37	30.96±1.24	44.87±0.58	24.17±1.81
60m	72.08±6.42	27.48±1.91	48.85±1.15	23.67±0.76

*The reaction performed at 90 °C for 1 h using 30 mg of 0.01Fe.0.01Ti-TUD-1 and 1:3 phenol:H_2O_2.

Table 4.5 Study of the catalyst recycling of bimetallic TUD-1

No. of Recycling	Conversion	Selectivity		
		HQ	CAT	BQ
#1	93.40±0.29	42.15±0.51	57.85±0.51	-
#2	24.88±2.40	20.53±2.03	32.20±1.08	47.27±2.78
#3	22.22±6.43	-	-	100±0.00

*The reaction performed at 90 ^{o}C for 1 h using 30 mg of 0.01Fe.0.01Ti-TUD-1 and 1:3 phenol:H_2O_2.

Table 4.6 Study of the hydrothermal stability of the catalysts

Sample	BET Surface Area (m^2/g)	Pore Volume (cc/g)	Average Pore Size (nm)
0.01Fe,0.01Ti-TUD-1 (Hydrothermal)	617	0.84	5.45
0.01Fe-TUD-1 (Hydrothermal)	674	0.93	5.54
0.01Ti-TUD-1 (Hydrothermal)	657	0.82	4.96
0.01Fe,0.01Ti-TUD-1 (3^{rd} Recycling)	529	0.90	6.80

*The reaction performed at 90 ^{o}C for 1 h using 30 mg of catalysts and 1:3 phenol:H_2O_2.

Table 4.7 Effect of the metal loading on phenol hydroxylation under UV irradiation

Sample	Conversion	Selectivity		
		HQ	CAT	BQ
TUD-1	11.08±2.94	-	9.81±0.90	90.19±0.90
0.01Fe-TUD-1	14.34±3.20	-	14.80±2.79	85.20±2.79
0.03Fe-TUD-1	14.81±1.23	-	-	100.00±0.00
0.01Ti-TUD-1	10.69±4.12	-	23.38±2.89	76.62±2.89
0.03Ti-TUD-1	14.87±0.42	-	11.25±1.03	88.75±1.03
0.05Ti-TUD-1	19.31±7.87	-	2.45±0.91	97.55±0.91
0.07Ti-TUD-1	19.76±2.65	-	1.03±0.53	98.97±0.53
0.09Ti-TUD-1	5.65±0.82	-	-	100.00±0.00
0.01Fe0.01Ti-TUD-1	17.35±1.73	-	11.00±0.91	89.00±0.91
0.01Fe0.03Ti-TUD-1	19.10±2.99	-	8.28±0.47	91.72±0.47
0.01Fe0.05Ti-TUD-1	14.66±5.86	-	3.27±0.30	96.73±0.30
0.01Fe0.07Ti-TUD-1	17.12±3.26	-	1.72±0.23	98.28±0.23
0.01Fe0.09Ti-TUD-1	7.08±1.98	-	2.33±0.73	97.67±0.73
0.03Fe0.01Ti-TUD-1	14.49±1.02	-	-	100.00±0.00
No H_2O_2	-	-	-	-
No catalyst	2.23±0.06	-	-	100.00±0.00

*The reaction performed under 100 W of UV radiation for 1 h using 30 mg of catalyst and 1:3 phenol:H_2O_2 ratio.

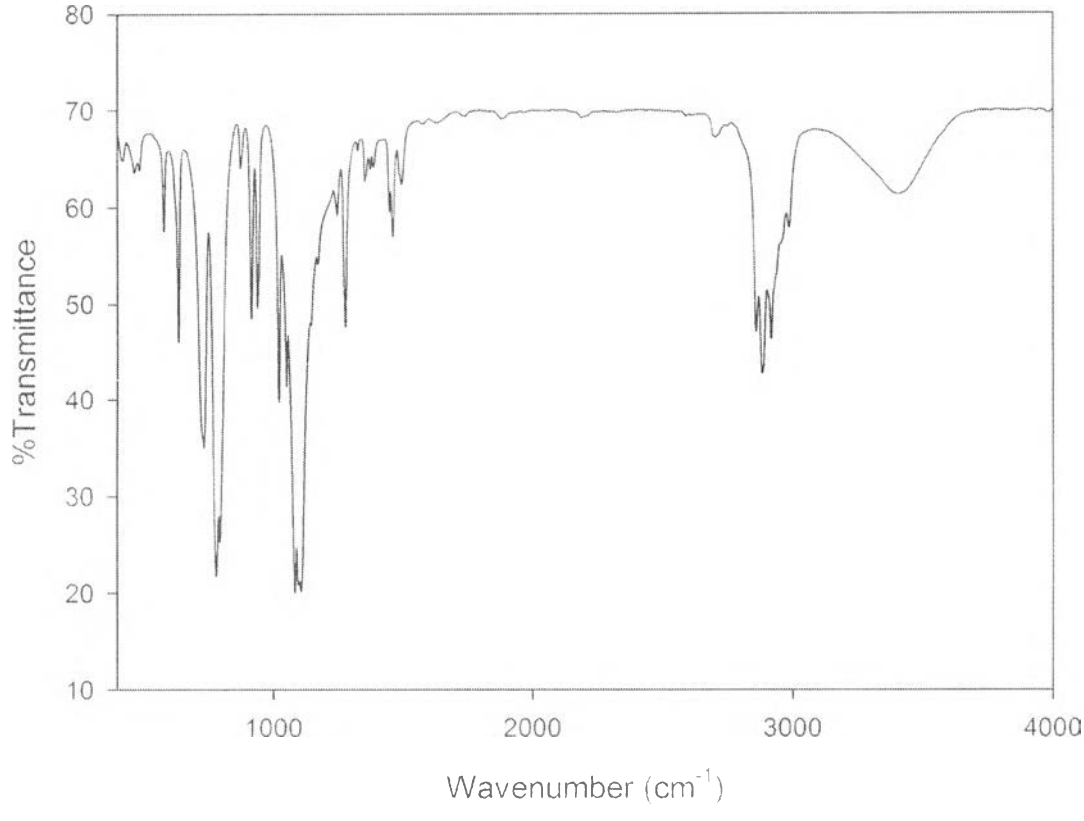

Figure 4.1 FTIR spectrum of silatrane precursor.

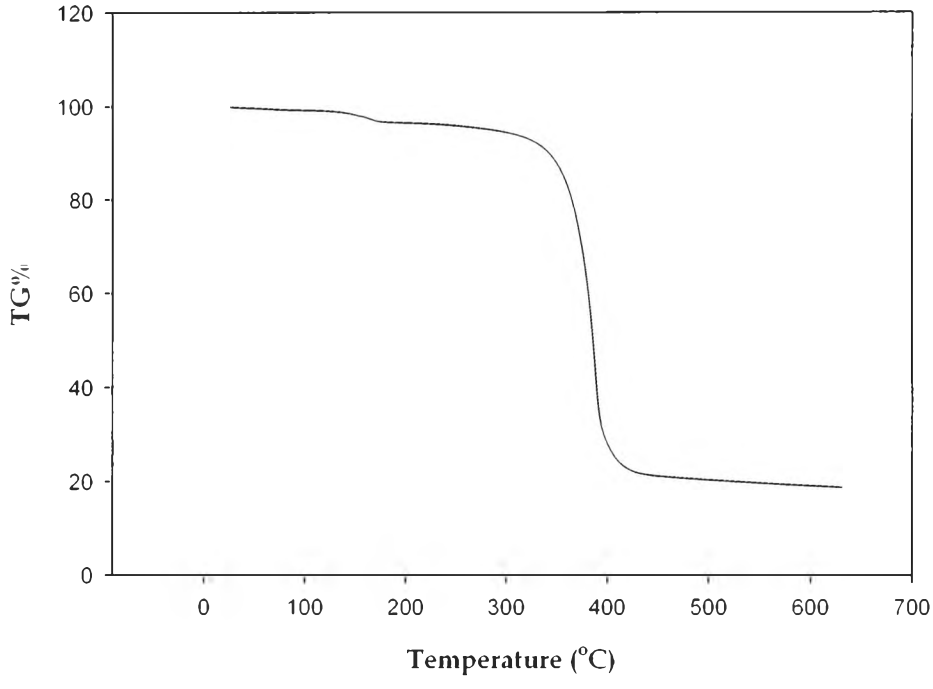

Figure 4.2 TGA thermogram of silatrane precursor.

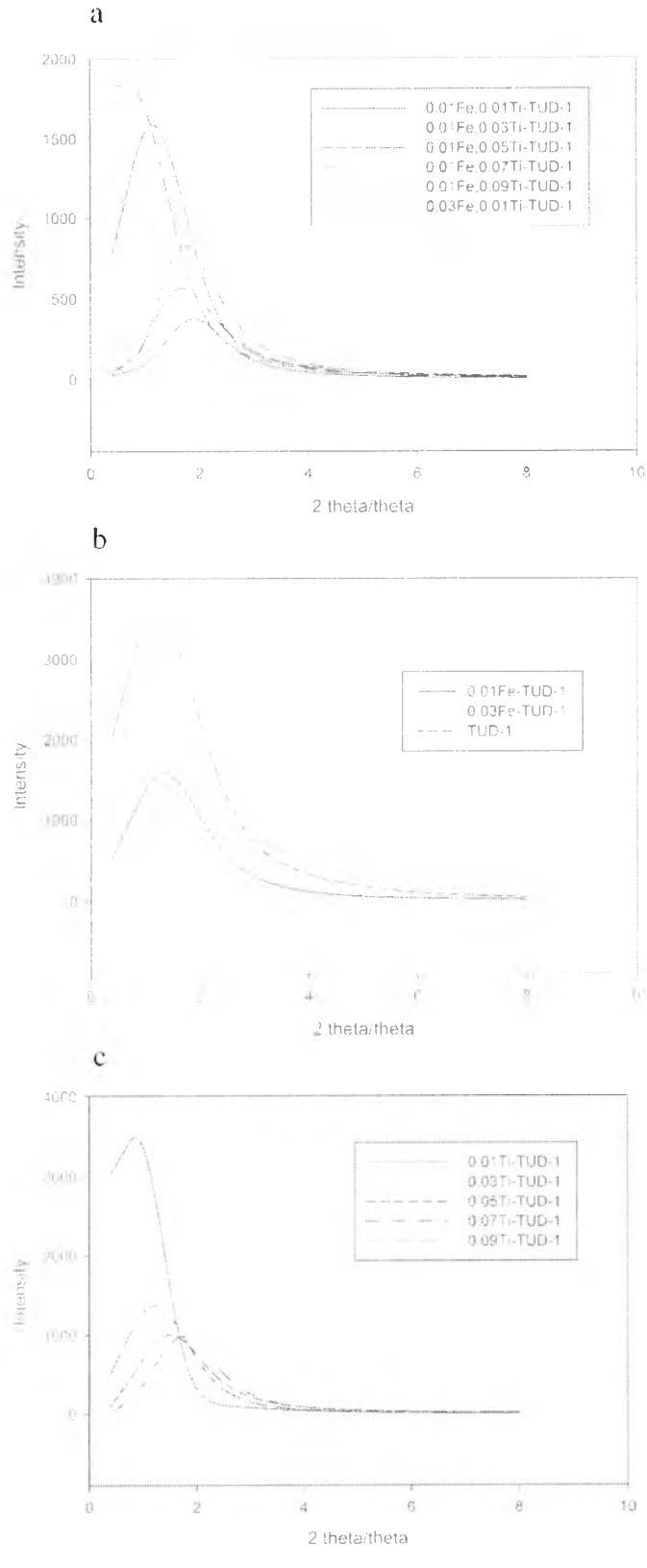

Figure 4.3 SAXD patterns of (a) Fe,Ti-TUD-1, (b) Fe-TUD-1 and (c) Ti-TUD-1.

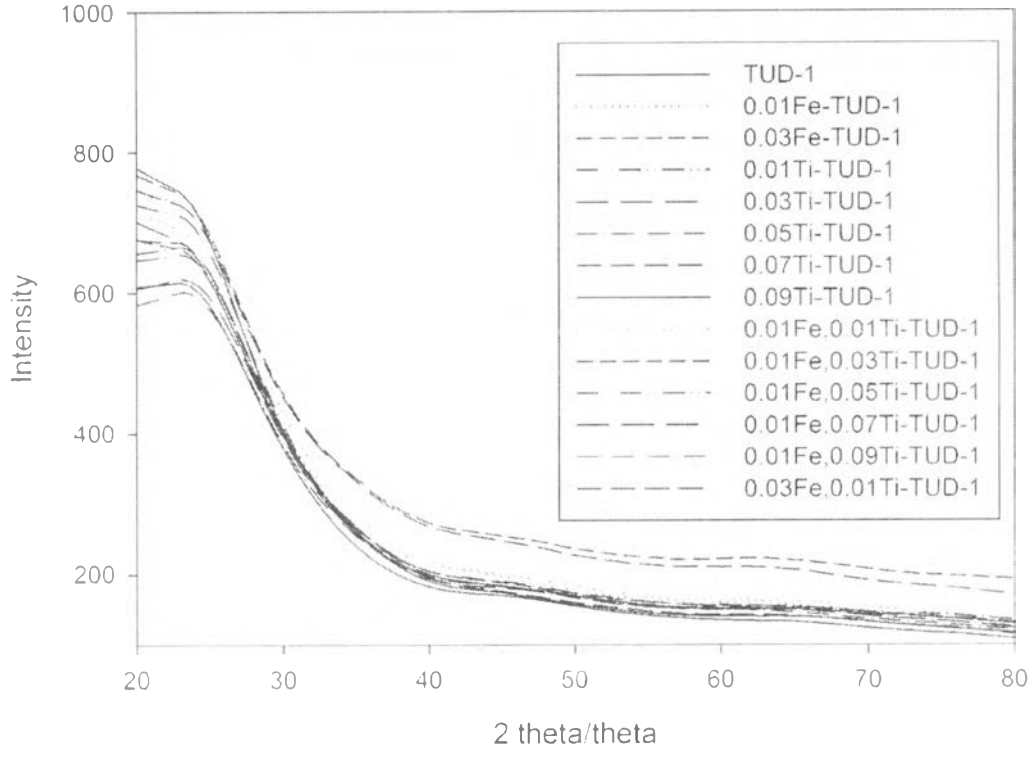

Figure 4.4 WAXD patterns of TUD-1, Fe-TUD-1, Ti-TUD-1 and Fe,Ti-TUD-1.

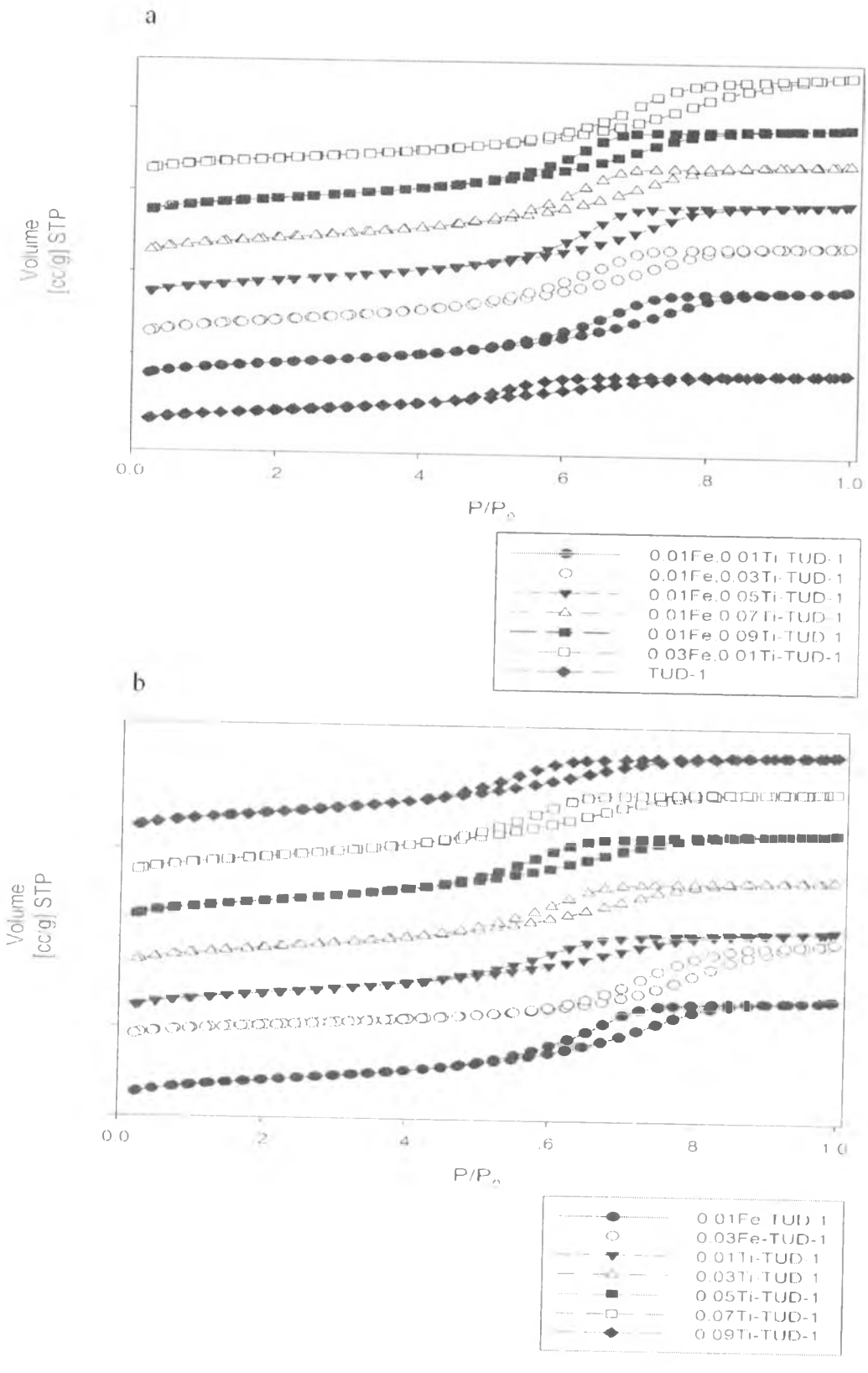

Figure 4.5 N_2 adsorption isotherms of (a) TUD-1 and Fe,Ti-TUD-1 and (b) Fe-TUD-1 and Ti-TUD-1.

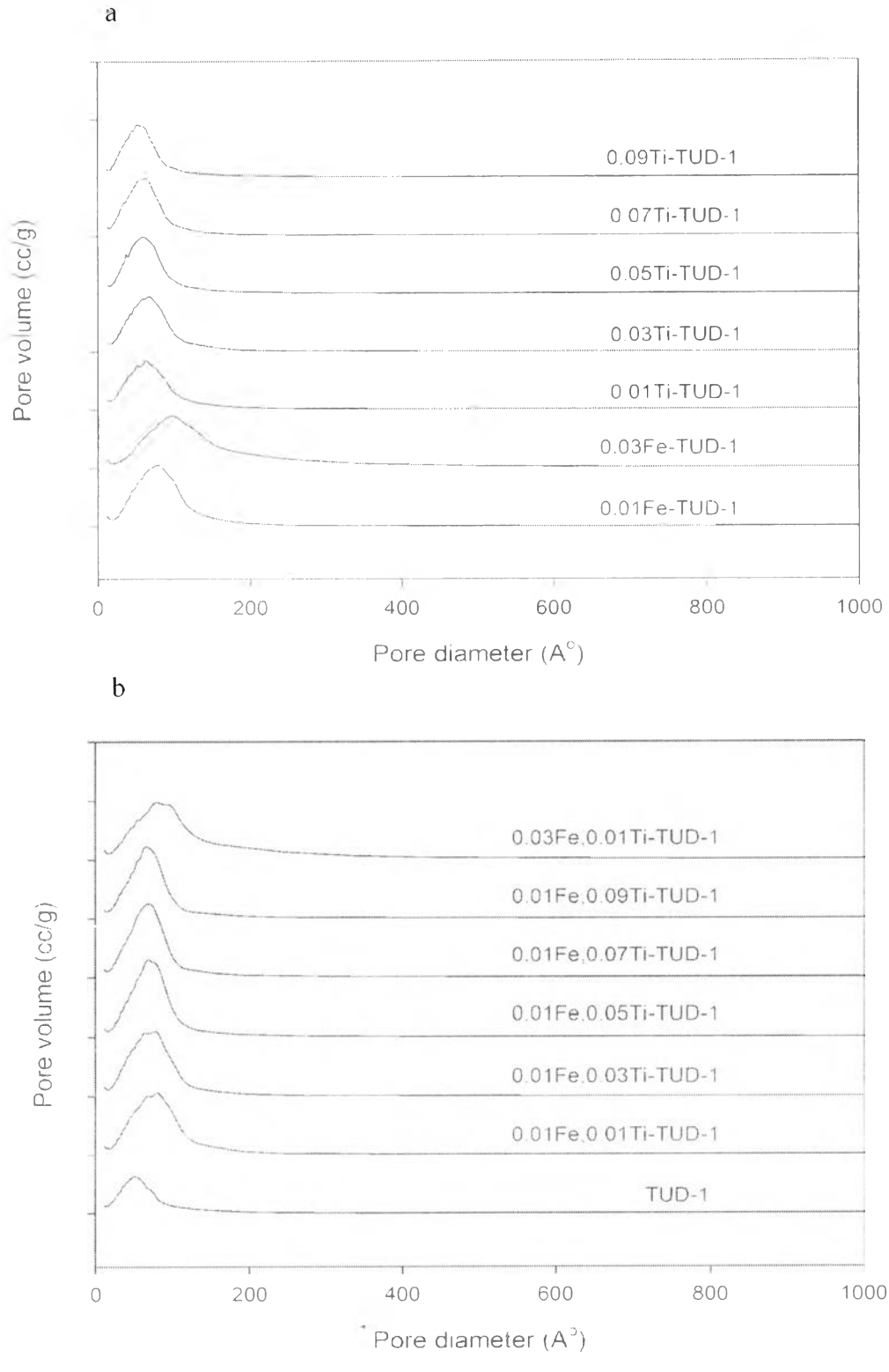

Figure 4.6 Pore size distributions of (a) Fe-TUD-1 and Ti-TUD-1 and (b) TUD-1 and Fe,Ti-TUD-1.

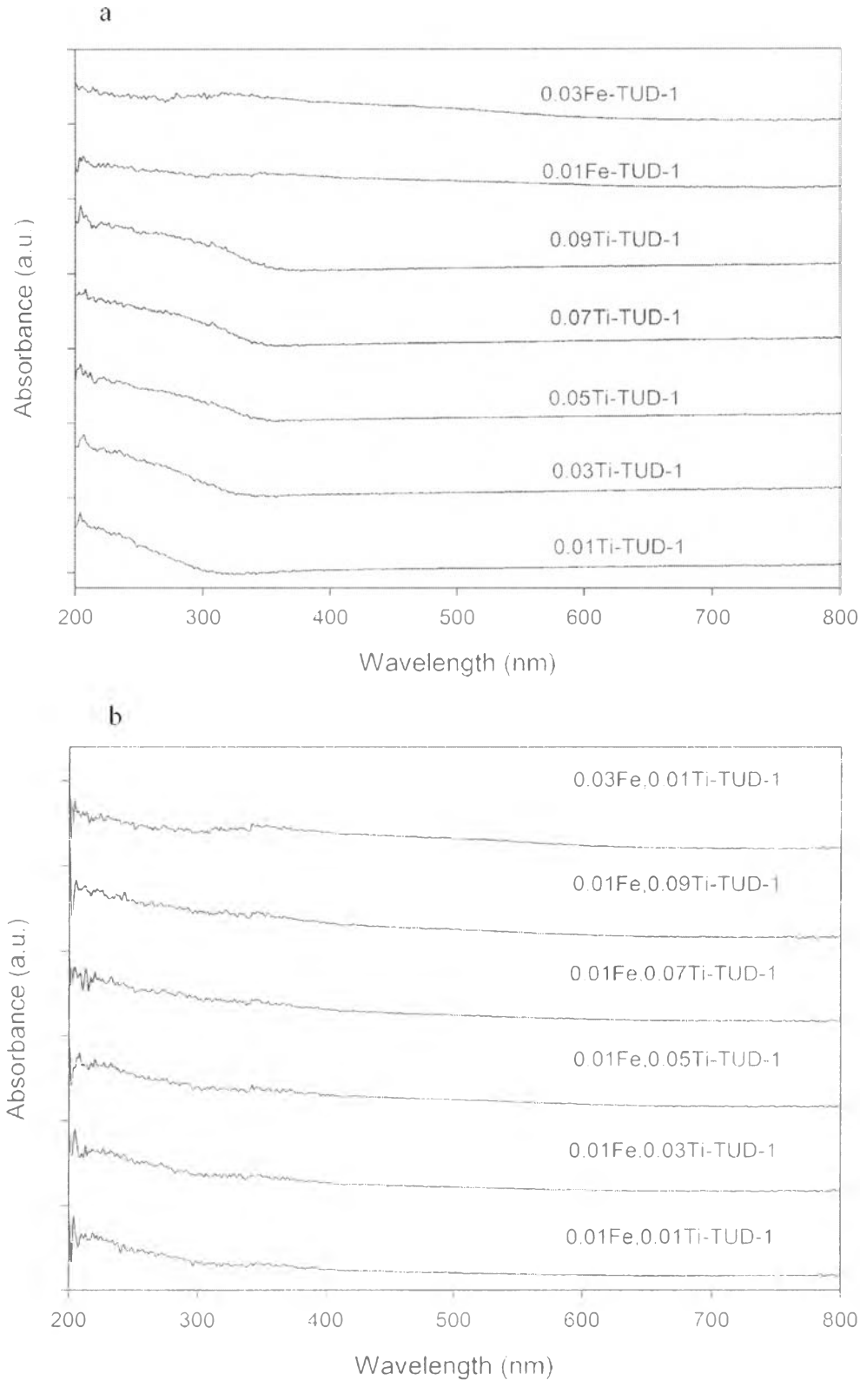

Figure 4.7 DRUV spectra of (a) Fe-TUD-1 and Ti-TUD-1 and (b) Fe,Ti-TUD-1.

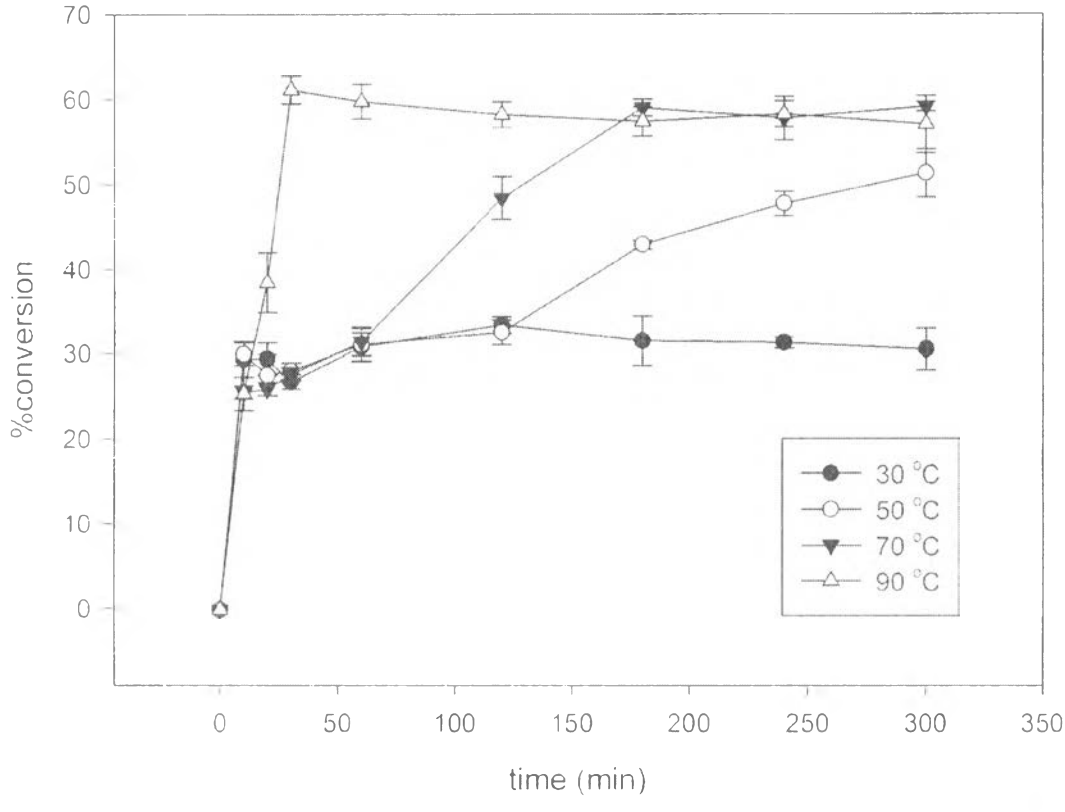

Figure 4.8 Effect of the reaction temperature on phenol conversion varied from 30 to 90 °C, using 30 mg of 0.01Fe.0.03Ti-TUD-1 and 1:1 phenol:H_2O_2 ratio.

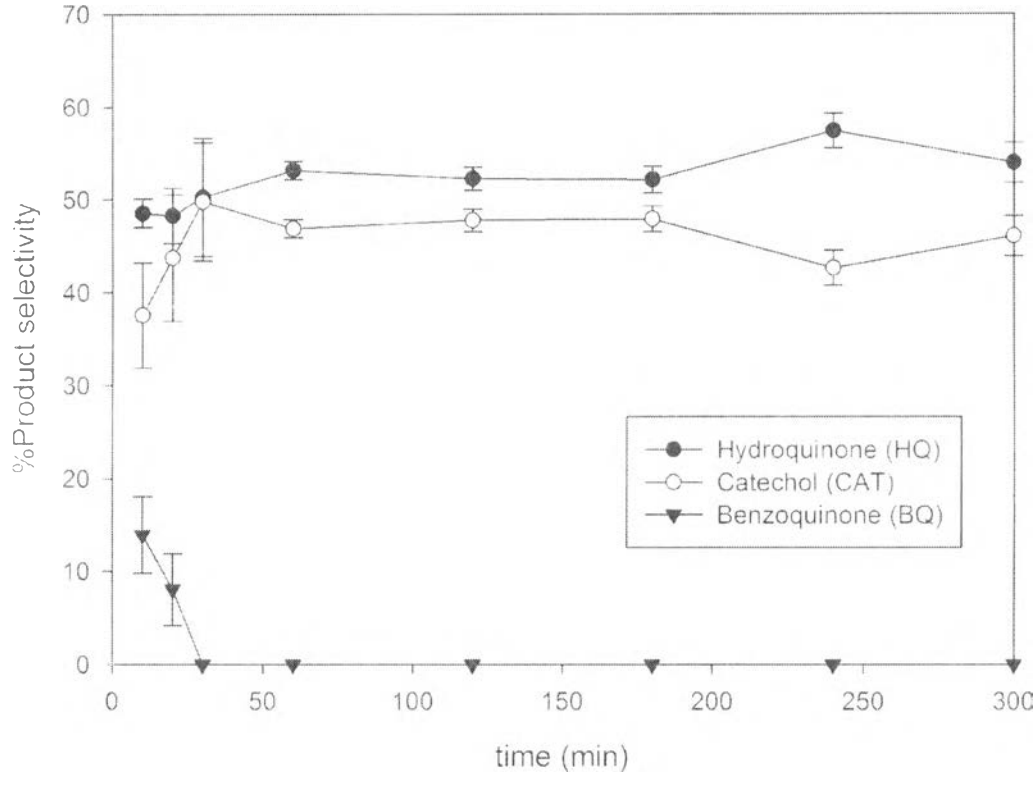

Figure 4.9 Effect of the reaction temperature on product selectivity performed at 90 °C, using 30 mg of 0.01Fe.0.03Ti-TUD-1 and 1:1 phenol:H_2O_2 ratio.

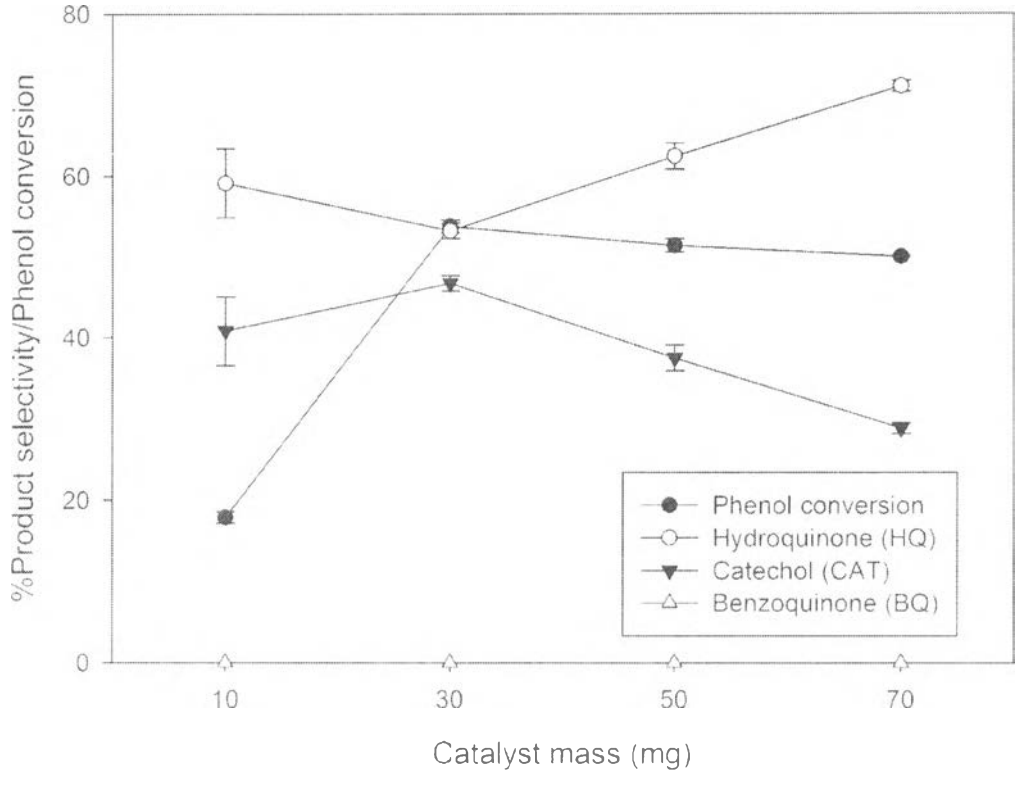

Figure 4.10 Effect of the catalyst content performed at 90 °C using 0.01Fe.0.03Ti-TUD-1 and 1:1 phenol:H_2O_2 ratio.

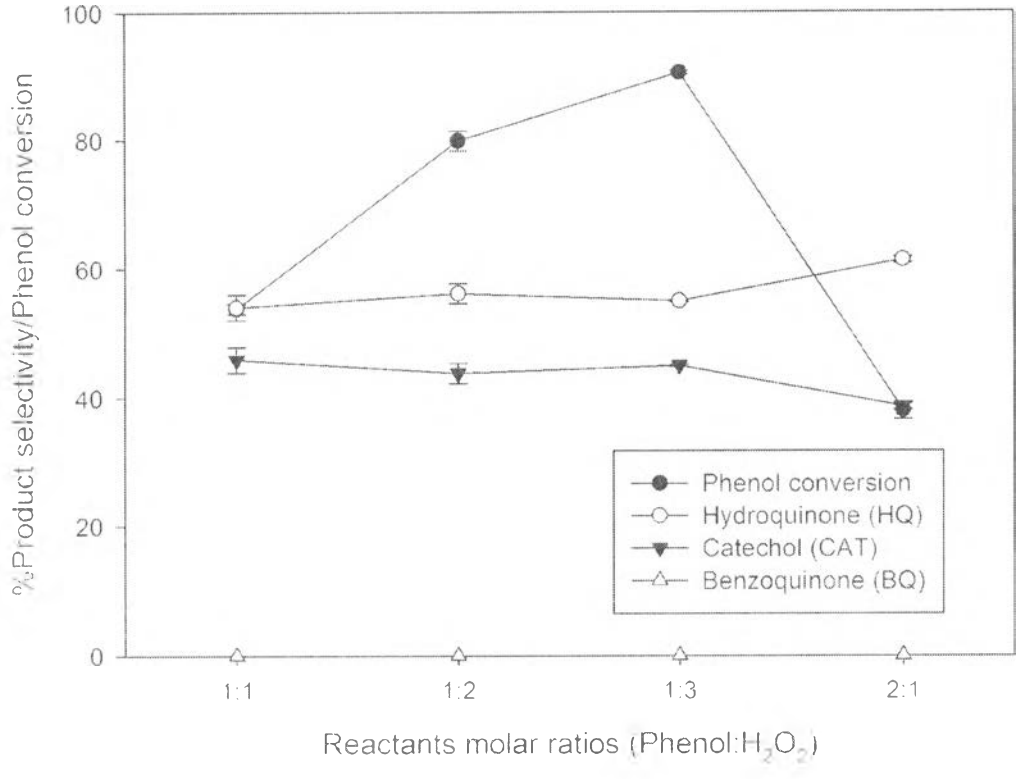

Figure 4.11 Effect of the reactants molar ratio performed at 90 °C using 30 mg of 0.01Fe.0.03Ti-TUD-1.

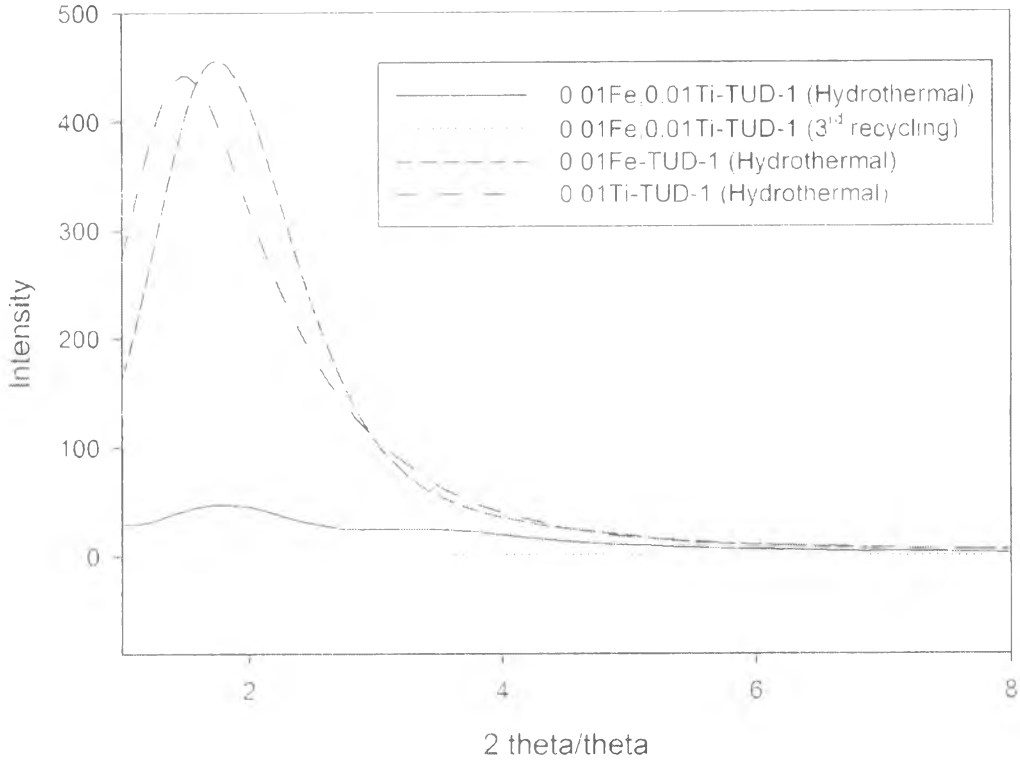

Figure 4.12 Study of hydrothermal stability of the catalysts.

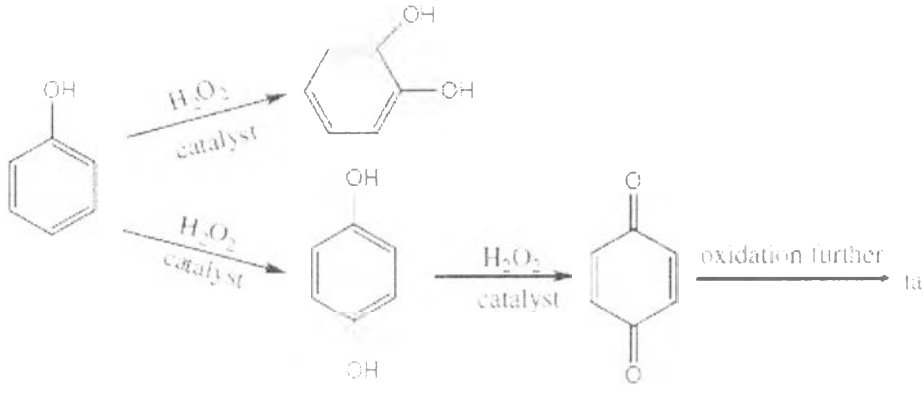

Scheme 4.1 Schematic of phenol oxidation [26].

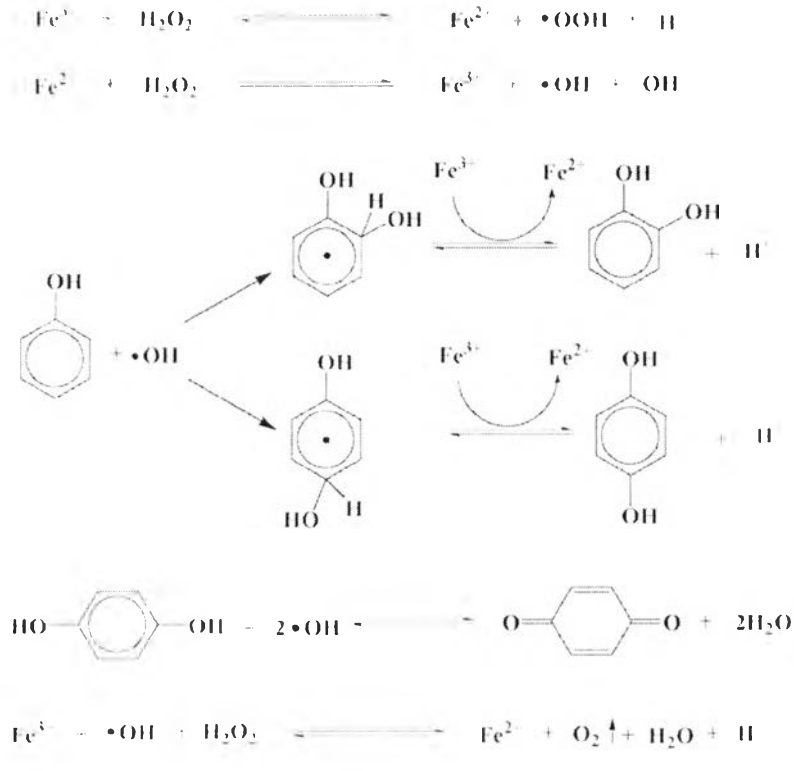

Scheme 4.2 Phenol hydroxylation reaction pathway of Fe ions [13].

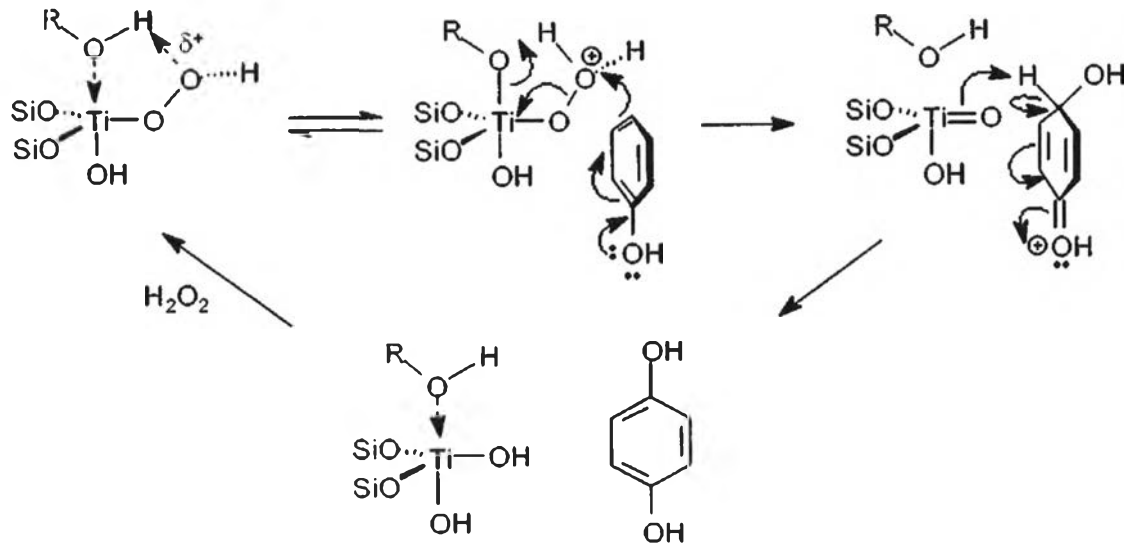

Scheme 4.3 Proposed reaction mechanism for the formation of HQ in phenol hydroxylation [27].

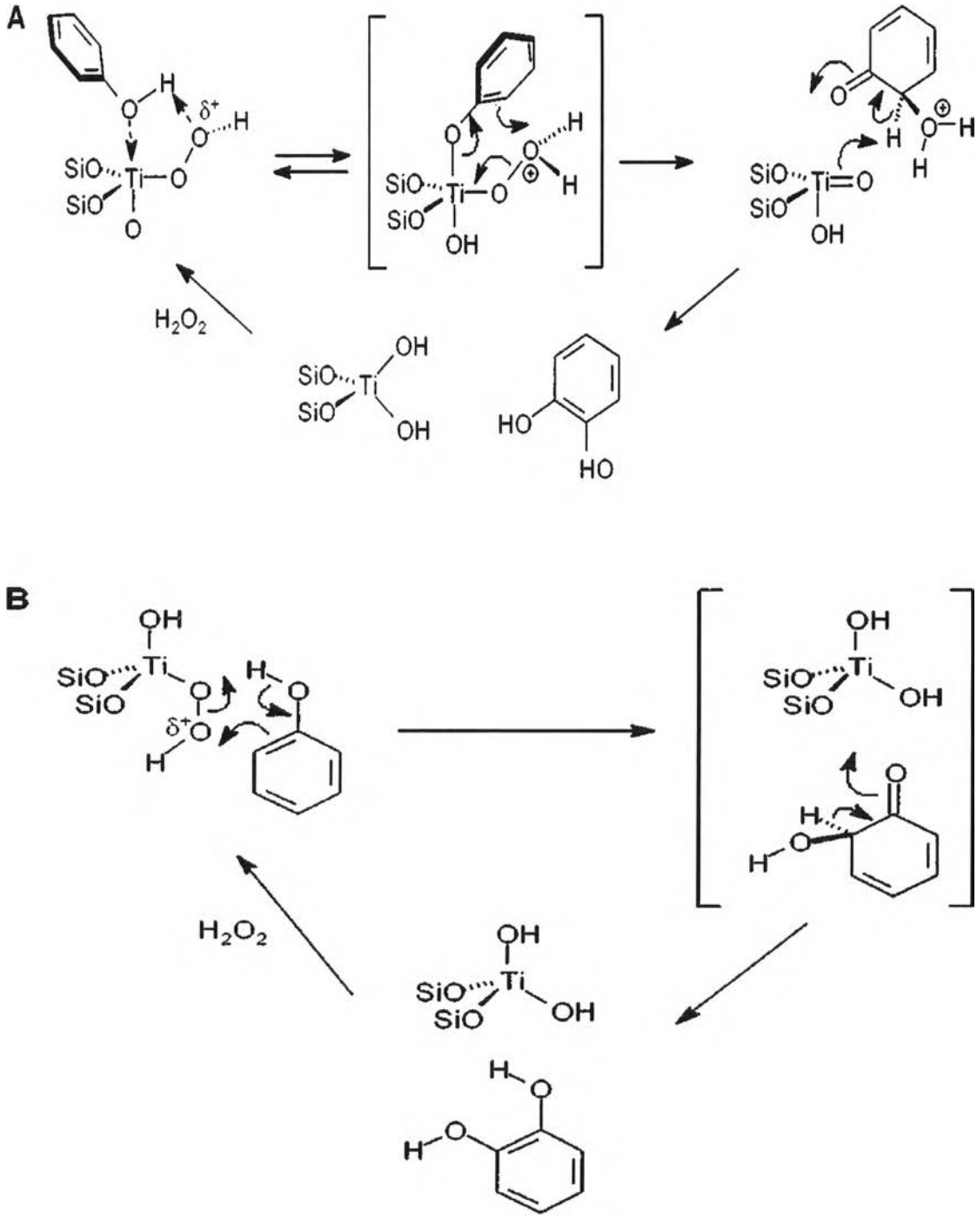

Scheme 4.4 Proposed reaction mechanism for the formation of CAT in phenol hydroxylation [27].